

Optical properties of bilayer InAs/GaAs quantum dot structures: Influence of strain and surface morphology

P. B. Joyce,¹ E. C. Le Ru,² T. J. Krzyzewski,¹ G. R. Bell,¹ R. Murray,² and T. S. Jones^{1,*}

¹Centre for Electronic Materials and Devices, Department of Chemistry, Imperial College, London, SW7 2AY, United Kingdom

²Centre for Electronic Materials and Devices, Department of Physics, Imperial College, London, SW7 2BZ, United Kingdom

(Received 1 October 2001; revised manuscript received 2 April 2002; published 7 August 2002)

Double layers of InAs quantum dots (QDs) separated by 112-Å GaAs spacer layers have been grown by molecular-beam epitaxy on GaAs(001) substrates. Photoluminescence measurements reveal that the emission of the second QD layer is blueshifted with respect to the first one. The two peaks can be made coincident by increasing the amount of InAs deposited in the second layer and also by annealing the spacer layer. Scanning tunnelling microscope measurements of the starting surface and of the uncapped QD's have been used to interpret these results. The QD's in the two layers are shown to have the same composition (pure InAs) before capping. However, QD's with similar shapes and volumes exhibit a blueshift in emission when grown in the second layer compared to a single layer. This is attributed to enhanced intermixing during the capping stage of the second-layer QD's, and is a consequence of these dots being more strain-relaxed due to the strain fields associated with the first QD layer. The blueshift is smaller for annealed spacer layers due to a lesser degree of strain relaxation as a result of the change of surface morphology induced by the annealing process.

DOI: 10.1103/PhysRevB.66.075316

PACS number(s): 68.37.Ef, 78.67.Hc

I. INTRODUCTION

Self-assembled InAs/GaAs quantum dots (QD's) are predicted to produce lasers with a low and temperature-independent threshold current.¹ The gain of a single QD layer is generally insufficient for lasing from the ground state (GS), and multiple layers of QD's emitting at the same wavelength are necessary. This is easily achieved by adopting relatively large spacer layers between the successive QD layers,² but this may not be the optimum design for some applications, in particular vertical cavity surface emitting lasers, where it is advantageous to have the layers grown closely spaced within the cavity. There have been several studies concerned with the electronic properties of multilayers of InAs/GaAs QD structures separated by thin spacer layers (<200 Å). In general, a redshift of the GS emission energy (with respect to the first layer) is observed, and this has been attributed to electronic coupling or tunnelling between successive QD layers.³⁻⁷ However, in some cases blueshifts have also been reported for InAs/GaAs (Refs. 2, 8, and 9) and Ge/Si QD's.¹⁰

Structural studies of multiple QD layers separated by thin spacer layers reveal that the growth of the second and successive layers is strongly affected by the underlying QD layer. Cross-sectional imaging techniques¹¹⁻¹⁵ revealed a strong tendency for vertical self-alignment of the QD's, and this has generally been attributed to the strain fields associated with the first QD layer providing a preferential nucleation site for QD's in the second and subsequent layers.^{11,16,17} We recently showed that during the growth of bilayer QD samples separated by thin (<200-Å) GaAs spacer layers, the critical coverage for QD formation (θ_{crit}) is reduced in the second layer by as much as 0.7-ML InAs deposition.¹⁸ This effect had also been observed for stacked Ge/Si QD's, emphasizing the similarities between the two systems.¹⁹ The reduction in θ_{crit} depends on a number of

factors including spacer layer thickness, and the rate and temperature at which the QD's are grown. However, θ_{crit} is not affected by an *in situ* annealing of the GaAs spacer layer prior to second-layer QD growth.¹⁸ This study also revealed large differences in the QD size and number density (N_s) when comparing growth on annealed and nonannealed spacer layers, and QD's grown in a single layer under identical conditions. The differences in N_s and size are expected to have a significant impact on the optical properties of encapsulated QD structures.

In this paper we present a detailed study of bilayer InAs/GaAs QD structures focusing on the optical and structural properties as determined by photoluminescence spectroscopy (PL) and scanning tunnelling microscopy (STM). PL measurements of bilayer samples separated by a relatively thin (112-Å), nonannealed GaAs layer show that the emission from the second layer is blueshifted with respect to the first one. Such an effect was already reported for the Ge/Si system¹⁰ and for InAs/GaAs QD's.^{2,20} We also show that it is possible to tune the second-layer emission by changing the InAs coverage, hence providing a simple method for producing coincident emission from the bilayer sample. We also demonstrate that annealing the spacer layer before growth of the second QD layer represents an alternative, more practical way of achieving coincident emission. Reflection high-energy electron diffraction (RHEED) and STM measurements demonstrate that the QD's have the same composition (pure InAs) before capping. However, QD's having similar shapes and volumes in the second layer exhibit a blueshift compared with the emission of a single layer. The blueshift is therefore attributed to enhanced intermixing during the capping stage for QD's of the second layer, a consequence of the second-layer QD's being more strain relaxed due to the strain fields associated with the QD's in the first layer. This interpretation was proposed and developed in Ref. 10 to explain similar results obtained for Ge/Si QD's, and it was suggested that similar considerations might also apply to III-V sys-

tems. Our PL and STM measurements confirm that the previous interpretation also applies to InAs/GaAs QD's, and in addition they show that the state of the surface plays a significant role.

II. EXPERIMENTAL DETAILS

The QD structures were grown in a purpose-built molecular-beam-epitaxy STM system (DCA Instruments/Omicron GmbH). RHEED intensity measurements of homoepitaxial growth on GaAs(001) and InAs(001) substrates were used to calibrate the Ga, In, and As₂ fluxes. Epiready GaAs(001) substrates (n^+ Si doped) were used for the growth of the QD samples. After initial thermal cleaning at 300 °C the native oxide layer was removed under an As₂ flux at 620 °C. A 0.5- μm GaAs buffer layer was grown at 580 °C and the substrate temperature then reduced to 510 °C. The samples were annealed under an As₂ flux for 5 min, and the surface exhibited a $c(4\times 4)$ RHEED pattern before InAs deposition.

The basic QD structure comprised two layers of InAs/GaAs QD's separated by a 112 Å GaAs spacer. In the following, the monolayer is defined relative to the InAs surface site density. The InAs growth rate was 0.016 ML s⁻¹, and the QD's were grown at 510 °C. The InAs coverage in the initial layer (θ_1) was fixed at 2.5 ML while the InAs coverage in the second QD layer (θ_2) was varied between 1.6 and 4.0 ML. The GaAs spacer layer was deposited at the same temperature as the first QD layer with a growth rate of 0.5 ML s⁻¹. RHEED was used to monitor θ_{crit} for QD formation. For this particular set of growth conditions, $\theta_{\text{crit}} = 1.9$ ML, and this was reduced for second layer QD growth by 0.5 ML.

Samples were also grown to investigate the effect of annealing the GaAs spacer layer prior to growth of the second QD layer. The duration of the annealing step was 10 min, and was performed at a temperature of 580 °C under an As₂ flux. After completion of the annealing stage the substrate temperature was reduced to 510 °C and allowed to thermally equilibrate prior to second layer InAs deposition. A $c(4\times 4)$ RHEED pattern was again observed. The introduction of the annealing step was found to have no effect on θ_{crit} for second layer QD growth, which again occurred at 1.4-ML InAs deposition.

Uncapped first and second layer QD's were imaged by STM. Upon completion of growth the samples were immediately transferred (within a few seconds) to the STM chamber and allowed to cool before imaging at room temperature. This approach is very effective in "freezing" the surface morphology and for obtaining atomic scale snapshots of the growth process.²¹ Constant-current STM images were obtained with a sample bias of -3.5 V and tunneling currents of 0.05–0.2 nA.

Samples were also grown for *ex situ* PL investigation. In this case the second-layer QD's were capped immediately with 400 Å of GaAs at 510 °C before the substrate temperature was increased to 580 °C for a final GaAs capping thickness of 1000 Å. PL measurements were made at low temperature (10 K) using an Ar⁺ or HeNe laser, dispersing the light with a SPEX 0.5-m monochromator and detecting with

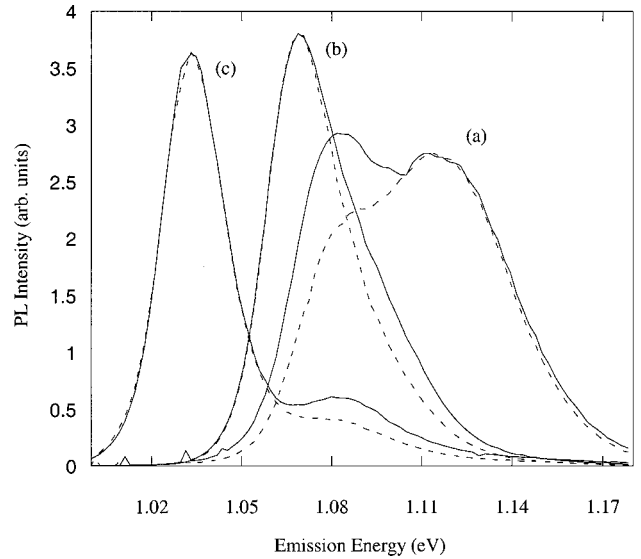


FIG. 1. Low-temperature PL spectra excited with a HeNe laser (solid lines) and an Ar⁺ laser (dashed lines) from bilayer QD samples with a nonannealed GaAs spacer of 112 Å, $\theta_1 = 2.5$ ML, and $\theta_2 =$ (a) 2.5, (b) 2.9, and (c) 3.7 ML, respectively.

a cooled Ge diode. In order to avoid any emission from the excited states, all the PL experiments were performed at low excitation densities.

III. RESULTS AND DISCUSSION

A. Optical properties

Low-temperature PL spectra of a capped single QD layer formed with $\theta_1 = 2.5$ ML ($\theta - \theta_{\text{crit}} = 0.6$ ML) shows emission at 1.08 eV with a linewidth of ≈ 40 meV. For a bilayer sample with $\theta_1 = \theta_2 = 2.5$ ML and a 420-Å GaAs spacer layer, the emission is practically indistinguishable from that of the single layer indicating that each QD layer is unaffected by the presence of the other (the spectrum is not included here). When the spacer layer thickness is reduced to 112 Å, two peaks are observed in the spectrum, indicating that the two layers emit at a different energy (excited-state emission is negligible at such low excitation). The spectrum is shown in Fig. 1(a). To identify the origin of each peak, we used variable pump wavelength PL (VPWPL).²⁰ This technique compares the emission spectra obtained from excitation with two lasers of different wavelengths (λ) and therefore different penetration depths. The shorter wavelength laser, in this case an Ar⁺ laser ($\lambda = 515$ nm), will favor emission from the upper layer compared to the HeNe laser ($\lambda = 632.8$ nm), which has a larger penetration depth. We can therefore attribute unambiguously the peak around 1.08 eV to emission from the first layer, and the higher energy peak at 1.12 eV to the second layer. The second layer is therefore strongly affected by the presence of the QD's in the first layer, resulting in a blueshift of the PL emission. By contrast, the first layer shows the same emission as a single QD layer and is not therefore affected by the presence of the second QD layer.

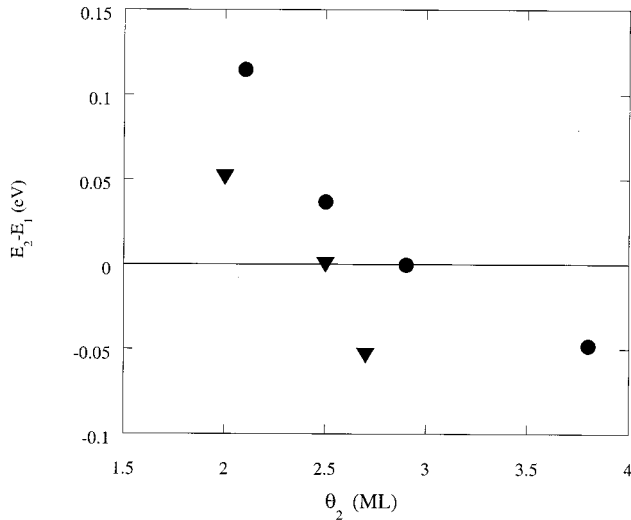


FIG. 2. Difference in emission energies of the second (E_2) and first (E_1) QD layers as a function of the second layer InAs coverage θ_2 for a fixed spacer of 112 Å. Increasing the InAs coverage in the second layer decreases the emission energy. The two curves intersect for $\theta_2=2.9$ ML in the case of the nonannealed spacer layer (circles) and at $\theta_2=2.5$ ML for the annealed spacer layer (triangles).

RHEED measurements reveal that θ_{crit} occurs at 1.4 ML in the second layer, compared with 1.9 ML for the first layer. If this change were the sole cause of the blueshift, we would expect that deposition of an equivalent amount of InAs after the two- to three-dimensional (2D \rightarrow 3D) growth mode transition for the second QD layer would result in a coincident emission peak in the PL spectra since the QD's should then contain the same amount of InAs. However, the PL spectra for a sample with $\theta_1=2.5$ ML and $\theta_2=2.0$ ML ($\theta - \theta_{\text{crit}} = 0.6$ ML in both layers), exhibit a greater peak separation with the second layer peak at an even higher energy. This is consistent with our previous work on single layers which showed that decreasing the InAs coverage blueshifts the QD PL emission.²² In order to make the two peaks coincident we have therefore deposited a greater amount of InAs in the second layer ($\theta_1=2.5$ ML, θ_2 variable). The first layer always emits around 1.08 eV, while the second layer shifts from 1.19 to 1.04 eV as θ_2 is increased from 1.9 to 4.0 ML (for a nonannealed GaAs spacer). Figure 2 shows a plot of the difference between the first- (E_1) and second-layer (E_2) QD emission energies for fixed θ_1 and different values of θ_2 . In the case of the nonannealed spacer layer coincident emission ($E_2 - E_1 = 0$) is achieved when $\theta_2=2.9$ ML [Fig. 1(b)]. Increasing θ_2 beyond this value increases the emission wavelength of the second layer beyond that of the first layer. An example is shown in Fig. 1(c), for which $\theta_1=2.5$ ML and $\theta_2=3.7$ ML. While obtaining coincident emission of several QD layers is of great importance for many applications, adjusting the InAs coverage of each layer to tune the emission is perhaps not practical for many layers, since the growth conditions vary from layer to layer.¹⁸ As an alternative, we have investigated the effect of annealing the surface of the spacer layer prior to growth of the second QD layer.

Figure 3 shows PL spectra of samples grown with θ_1

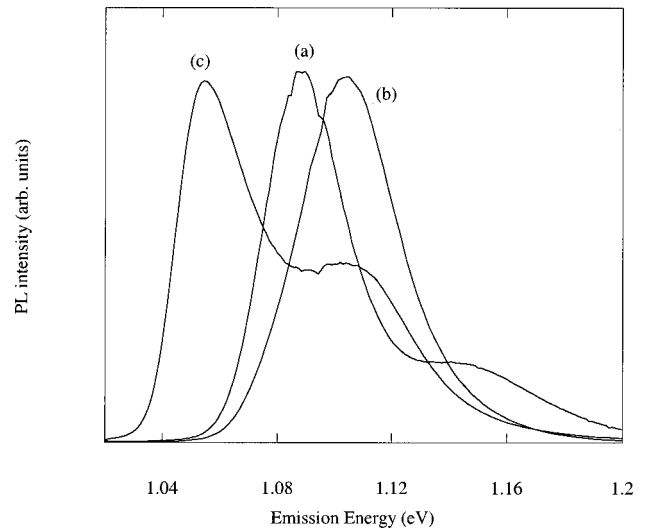


FIG. 3. Low-temperature PL spectra from bilayer QD samples with an annealed GaAs spacer of 112 Å, $\theta_1=2.5$ ML, and θ_2 = (a) 2.0, (b) 2.5, and (c) 2.7 ML.

= 2.5 ML and three values of θ_2 . In each case the GaAs spacer layer was annealed at 580 °C for 10 min before deposition of the second QD layer. As mentioned in Sec. II, θ_{crit} is not affected by annealing and still occurs at 1.4 ML for the second layer in these samples. VPWPL is again used to identify the emission from samples exhibiting two peaks. In this case, coincident emission is obtained for $\theta_1 = \theta_2 = 2.5$ ML [Fig. 3(b)], while values of $\theta_2 = 2.0$ and 2.7 ML produce two separate PL peaks [Figs. 3(a) and 3(c)]. Spacer layer annealing is hence demonstrated as a simple way to achieve coincident emission for QD bilayers in the present growth conditions. For $\theta_1 = 2.5$ ML and $\theta_2 = 2.0$ ML, the same amount of InAs has been deposited after the 2D \rightarrow 3D transition in both layers ($\theta - \theta_{\text{crit}} = 0.6$ ML), due to the reduction of θ_{crit} by 0.5 ML in the second layer. In this case, the emission of the second layer is again blueshifted compared to the first layer, similar to the results obtained for the nonannealed spacer layer [Fig. 1(a)]. The difference in PL peak energies of the two QD layers ($E_2 - E_1$) is also shown in Fig. 2 for annealed spacers as a function of θ_2 . Just as for the nonannealed spacer layers, increasing the InAs coverage results in a decrease in the emission energy (E_2), reaching 1.04 eV at $\theta_2 = 2.7$ ML. The emission energy (E_2) for annealed spacer layers is always lower than that measured for nonannealed spacers for comparable values of θ_2 .

An aspect common to the growth of second layer QD's on unannealed and annealed spacer layer samples is the reduction in the amount of InAs required for the 2D \rightarrow 3D growth mode transition. This should imply a thinner or incomplete wetting layer (WL). A similar effect has been observed for Ge/Si QD's.^{10,19} To investigate this in more detail we studied the emission from WL's under conditions of high excitation. Such a spectrum is shown in the inset to Fig. 4 for the sample with $\theta_1 = \theta_2 = 2.5$ ML and an unannealed spacer layer. The shape of this spectrum suggests the presence of two overlapping features, which we tentatively attribute to emission from the WL's associated with each QD layer of the

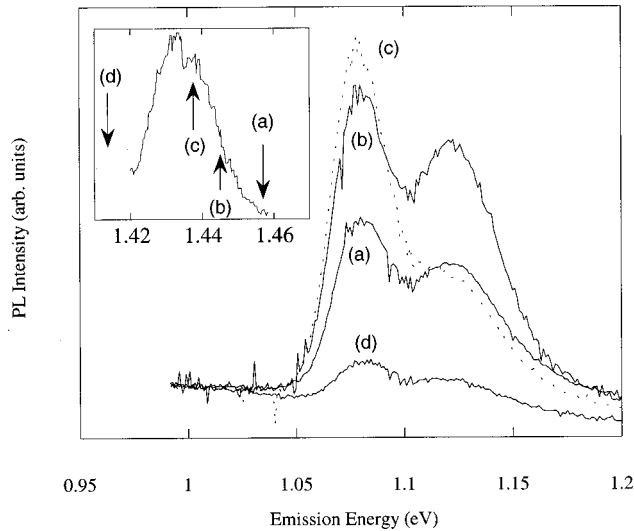


FIG. 4. Low-temperature PL spectra obtained for the nonannealed bilayer QD sample with nominally identical layers ($\theta_1 = \theta_2 = 2.5$ ML) at excitation energies of (a) 1.458, (b) 1.446, (c) 1.438, and (d) 1.414 eV. Spectra (a), (b), and (d) exhibit roughly equal contributions from each QD layer, whereas the first layer dominates in spectrum (c) (dashed line). In this case, the excitation energy is below the absorption edge of the second WL. The inset shows the PL spectrum in the region of the WL for nonresonant excitation (Ar^+ laser); the arrows indicate the excitation energies for each resonant PL spectrum.

bilayer structure. To confirm this, we collected the PL signal from the QD's when resonantly exciting at energies between 1.414 and 1.458 eV. Some of the spectra obtained are presented in Fig. 4. Spectrum (a) corresponds to excitation above both WL's band edges and emission from both QD layers is present. Decreasing the excitation energy results in an increase in the QD emission (a)–(c) followed by a decrease (d). However, the emission from each QD layer does not reach its maximum intensity for the same excitation energy. Spectrum (b) corresponds to the maximum of the second QD layer while (c) corresponds to the maximum for the first. Note that emission from the second layer has almost disappeared in spectrum (c), represented as a dashed line in Fig. 4, demonstrating that an energy of 1.438 eV is below the absorption edge of the second-layer WL but not of the first. Decreasing the excitation energy below both WL's produces only direct absorption into the QD's, and hence a strong reduction in the PL intensity; this is shown in spectrum (d). From this series of spectra, we can conclude that the energy of the second WL is slightly higher (≈ 8 meV) than that of the first layer consistent with it being thinner. We can also note a small difference between the maximum of absorption and the maximum of emission (Stokes shift) for each WL of the order of 7 meV. Finally, this study of the WL's shows that it is possible to selectively excite one of the layers using resonant excitation, confirming the absence of significant electronic coupling and tunneling.

B. STM analysis

To investigate the differences in PL emission from the bilayer QD structures we have performed STM measure-

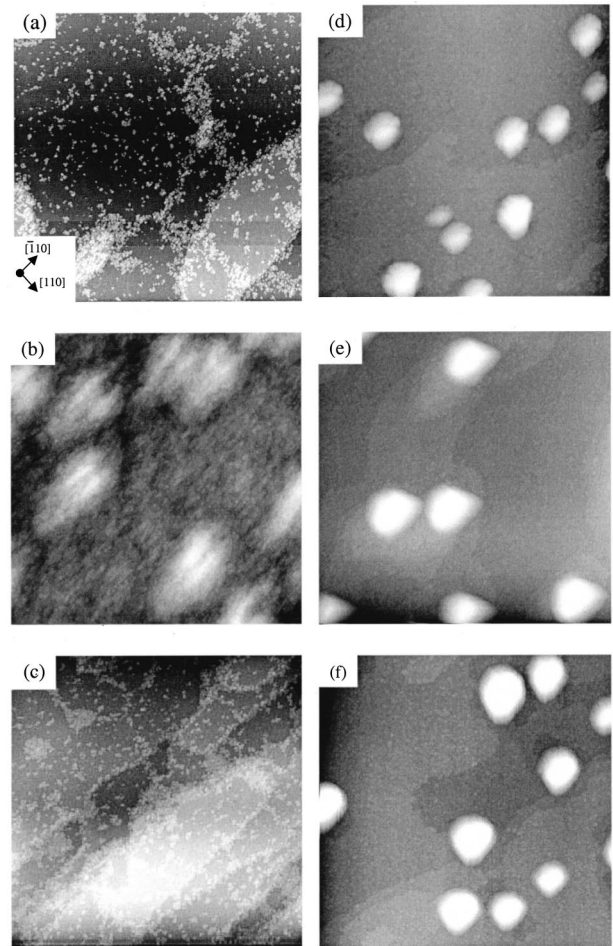


FIG. 5. Filled-states STM images ($2000 \times 2000 \text{ \AA}^2$) showing the GaAs surface morphology prior to deposition of InAs; (a) first layer, (b) second layer with a nonannealed 112-Å spacer, and (c) second layer with an annealed 112-Å spacer. Images (d)–(f) show the QD morphology after 2.5-ML InAs deposition; (d) first layer, (e) nonannealed GaAs spacer layer, and (f) annealed GaAs spacer. The InAs coverage in the first layer was fixed at 2.5 ML for (b), (c), (e), and (f).

ments on uncapped single QD layers and second-layer QD's grown on both nonannealed and annealed GaAs spacer layers (112 Å). We also present STM images of the GaAs surface prior to InAs deposition to highlight the differences in surface morphology, which may affect the subsequent growth of the QD layers.

The STM topographs in Figs. 5(a)–5(c) compare the GaAs starting surface for QD growth in both single- and double-layer structures. The surface morphology prior to deposition of the first layer of QD's ($\theta_1 = 0$) is shown in (a). It is characterized by a number of small monolayer high islands together with much larger regions which exhibit a $c(4 \times 4)$ reconstruction.²³ The image in (b) is characteristic of the surface used for growth of the second layer of QD's ($\theta_2 = 0$) after the initial QD layer ($\theta_1 = 2.5$ ML) has been overgrown with 112 Å of GaAs at 510 °C. No post-growth annealing has been performed, and high-resolution images show a 2×4 reconstruction. There is no evidence of a 1×3 phase, a surface reconstruction associated with the pres-

ence of an $\text{In}_x\text{Ga}_{1-x}\text{As}$ surface alloy,²⁴ so significant In segregation through the 112-Å spacer layer can therefore be ruled out.

Much more important differences arise in the larger scale morphology of the second layer surface compared to the first layer. Figure 5(b) shows the presence of mounds that are a consequence of GaAs overgrowth on top of the initial layer of QD's. For this GaAs thickness, the average height of the mounds is 27 Å and the lateral dimensions are typically 300 Å (along [110]) by 500 Å (along $[\bar{1}10]$). The mounds are also characterized by a valley (depression) running through their center and along $[\bar{1}10]$. The average valley depth in this case is 9 Å, although this varies significantly with the GaAs thickness.²⁵ We recently characterized the overgrowth process in detail using STM, and showed that valleys only form during overgrowth of the relatively large QD's formed at low InAs growth rates. The development of the valley at the top of the mounds reflects the anisotropic migration of Ga adatoms away from the top of the QD due to a combination of stress and surface curvature. It should also be noted that, although 3D features are still observed on the surface, the QD's are fully encapsulated at a capping layer thickness of 112 Å.²⁵

Figure 5(c) shows the starting surface for second layer QD growth after the surface has been annealed for 10 min at 580 °C and then allowed to cool down to 510 °C under an As_2 flux. The surface is similar to that observed for growth of the first layer [Fig. 5(a)]. The annealing cycle allows the spacer layer to minimize its surface energy and flatten via adatom migration; the effect of surface stress on adatom migration is clearly very small at this cap thickness.^{25,26}

The STM images in Figs. 5(d)–5(f) were recorded after deposition of 2.5-ML InAs on each of the surfaces shown in Figs. 5(a)–5(c), respectively. QD's are formed in all cases since $\theta > \theta_{\text{crit}}$. Dots in the first layer (d) are present at a density of $N_s \approx (1.7 \pm 0.1) \times 10^{10} \text{ cm}^{-2}$ with an average volume of $1.56 \times 10^6 \text{ Å}^3$. For growth on the annealed spacer layer (f) N_s is almost identical to the first layer, but the mean QD volume is greater by a factor of about 2. By contrast, second-layer growth on the nonannealed spacer layer (e) leads to a reduction in N_s to $8.3 \times 10^9 \text{ cm}^{-2}$ and to a greater average QD volume of $4.67 \times 10^6 \text{ Å}^3$. There are also clear differences in the QD nucleation sites. In the case of the annealed spacer layer and the single-layer samples [(f) and (d)] QD nucleation occurs at the bottom of step edges, whereas on the nonannealed spacer layer (e) the islands nucleate exclusively at the top of the mounds that exist as a consequence of GaAs overgrowth on top of the initial layer of QD's.²⁵

The average volume of both the first and second layer QD's can be determined by direct integration of the STM images and is plotted in Fig. 6(a) as a function of $\theta - \theta_{\text{crit}}$. When the change of critical thickness in the second layer is accounted for in this way, the average volumes of the QD's in the first- and second-layer QD's grown on the annealed thin spacer layer (112 Å) are identical, whereas the average volume for the QD's grown on the nonannealed spacer layer is significantly greater. The QD volume increases at a rate of

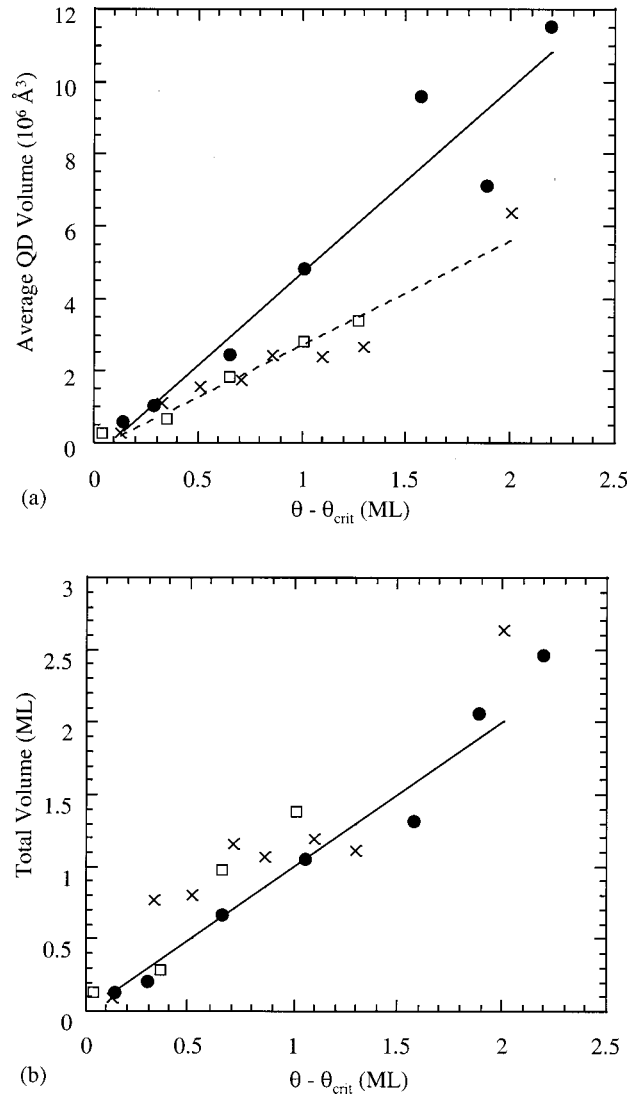


FIG. 6. (a) Mean QD volume determined by STM as a function of InAs coverage ($\theta - \theta_{\text{crit}}$) for the QDs in the different layers of the bilayer structure: first layer (\times), second layer with a nonannealed spacer (\bullet), and second layer with an annealed spacer (\square). (b) Total QD volume per unit area (in ML equivalents) as a function of ($\theta - \theta_{\text{crit}}$) for the different QD structures; symbols as above. The solid line is that expected for Stranski-Krastanov (SK) growth without any $\text{In}_x\text{Ga}_{1-x}\text{As}$ alloying.

$5.1 \times 10^6 \text{ Å}^3 \text{ ML}^{-1}$ for QD's grown in the second layer on a nonannealed spacer layer compared to $2.8 \times 10^6 \text{ Å}^3 \text{ ML}^{-1}$ for those in the first layer and when grown on the annealed spacer layer. The data are summarized in Table I.

The differences observed relate to the measured changes in N_s . To take into account the change in density and in order to extract compositional information, the total volume per unit area of the QD's, V , in ML equivalents, is plotted in Fig. 6(b), over a range of coverages beyond θ_{crit} for the three different types of samples. The solid line $V = \theta - \theta_{\text{crit}}$ represents the expected volume for simple Stranski-Krastanov (SK) growth, i.e., no incorporation into the QDs of WL material and no alloying.^{22,27} In all three cases, there is little deviation from the SK line, showing that the QD composi-

TABLE I. Summary of results obtained from STM images of uncapped InAs/GaAs QD's: the number density N_s , critical thickness θ_{crit} and rate of increase of mean volume $\langle V \rangle$ of the QD's with InAs coverage θ . The latter parameter is a measure of the QD evolution which is not sensitive to any change in θ_{crit} .

	N_s (10^{10} cm^{-2})	θ_{crit} (ML)	$d\langle V \rangle/d\theta$ ($10^6 \text{ \AA}^3/\text{ML}$)
single/first layer	1.7	1.9	2.8
second layer, non-annealed spacer	0.8	1.4	5.1
second layer, annealed spacer	1.6	1.4	2.8

tion is therefore close to 100% InAs. This is expected for the low growth rate conditions used here to form the QD's.²⁷ Compositional differences in the *uncapped* QD's cannot be used therefore to explain the observed differences in PL emission (Sec. III A), and an alternative explanation is required.

C. Wetting layers and critical thickness

A reduction in the critical thickness for stacked QD's has previously been reported for Ge/Si QD's.^{10,19} The comparison between annealed and nonannealed spacer layers enables us to clarify the origin of this effect for InAs/GaAs QD's. Indeed, the critical thickness θ_{crit} is smaller in the second layer by 0.5 ML whether the 112-Å spacer layer is annealed or not. Since annealing at high temperatures is expected to desorb any surface-segregated In, this indicates that the change of θ_{crit} is caused solely by the strain fields of the buried QD's and not by any effects arising from In segregation. It is also clear that the change of spacer layer morphology with annealing [compare Figs. 5(b) and 5(c)] does not contribute to the change of θ_{crit} . The second WL emission occurs at an energy ~ 8 meV higher than the first (Fig. 4), consistent with a smaller In content alloyed WL spread over a few atomic layers. The reduction of θ_{crit} means that an extra 0.5 ML of InAs is incorporated into the second-layer QD's if the same amount of material is deposited overall, and this substantially increases the average QD volume. It may also affect the composition of the layer directly surrounding the buried QD's, since it is known that the WL tends to spread upward into more of a "confining layer" under the present capping conditions.²⁸

D. Nonannealed spacer layer

The number density of QD's in the second layer is smaller than in the first layer, while the QD average volume increases at a correspondingly greater rate (Table I). The reduction in number density is a consequence of the different surface morphology.¹⁸ The growth is still SK-like and the composition of the uncapped QD's is close to pure InAs, as in the first layer. However, despite the greater average QD volume, the PL emission is blueshifted ($E_2 - E_1 > 0$) compared to the first-layer QD's for the same coverage beyond θ_{crit} (Fig. 2). Of course, one would expect that the emission

from QD's with larger volume and identical composition is redshifted, and indeed increasing the volume of the second-layer QD's leads to a redshift, allowing a "tuning" of the emission energy (Fig. 2). This means that there is a competing mechanism for the second-layer QD's causing a blueshift relative to similar-sized QD's in the first layer. Either compositional differences *after* capping, or differences in the strain state of the QD's, could account for this change, and these are discussed in Sec. III F.

E. Annealed spacer layer

Unlike the nonannealed spacer layer, growth on the annealed spacer results in a QD density similar to the first layer. Again the QD's are larger than in the first layer, but this time the size difference is only related to the change of critical thickness, i.e., the QD's are approximately the same size as those grown in the first layer with 0.5 ML more coverage. For the same coverage in the second layer as the first, the second-layer QD's emit at a similar energy to those in the first layer, as shown in Figs. 2 and 3. This is despite the larger average size of the second-layer QD's. Also, relative to second-layer QD's grown on a nonannealed spacer layer, these QD's have a lower emission energy at the same coverage (Fig. 2). This means that the blueshifting mechanism operating for second-layer QD's with a nonannealed spacer also operates in this case, although it is weaker for the annealed spacer layer. This provides an additional method for "tuning" the second-layer QD emission energy.

F. Strain and composition effects

The results presented above provide us with a means of probing the effect of strain and intermixing during the capping stage. Three types of QD's have been grown: dots in a single layer (type I), dots in a second layer deposited on an unannealed GaAs spacer (type II), and dots in a second layer on an annealed GaAs spacer (type III). Characterization with STM and RHEED has shown a number of differences. The density is reduced for type-II dots due to the different surface morphology, and QD formation occurs earlier for type-II and -III dots due to the strain field from the underlying first-layer dots. As a result, for identical InAs coverages ($\theta = 2.5$ ML), type-II dots are larger than type-III dots and both are larger than type-I dots. An important result is that the composition of all three types of dots is the same and close to pure InAs *before capping*. Also, by changing the amount of In deposited in the second layer, it is possible to obtain QD's of types II and III with the same average volume as QD's of type I. For example, if $\theta = 3.1$ ML ($\theta - \theta_{\text{crit}} = 1.2$ ML) for type I dots, we need $\theta = 1.4 + 1.2/2 = 2.0$ ML for type-II dots and $\theta = 1.4 + 1.2 = 2.6$ ML for type-III dots. These three QD's then have the same average volume and the same In composition. Furthermore, no significant differences in the shape of the dots were observed in the STM images. The only difference between these three cases prior to capping is the strain state of the islands. However, the PL emission of the capped dots show major differences, with emission from type-III dots blueshifted compared to type-I dots, and an even larger blueshift observed for type-II dots.

We therefore conclude that the strain state of the dots before capping has an important effect on the structure of the capped dots.

It has been shown that uncapped QD's are partially strain relaxed (i.e., have a lattice constant larger than GaAs), the largest strain relaxation occurring at the top of the QD.²⁹ The deposition of GaAs will tend to force the lattice constant back to that of GaAs, and the resulting buried QD's are more strained than before capping but may still be partially strain relaxed in their center. When QD's grow on top of an existing QD layer, the strain field from the buried QD can extend to the surface of the spacer layer (depending on its thickness) and introduce regions of tensile strain directly above a QD. This strain modulation is believed to be the cause of QD vertical self-alignment and the reduction in θ_{crit} .^{11,17,18} It is likely that QD's forming on these regions will be more strain relaxed, because the surface is already subjected to tensile strain. We might expect that these QD's (types II and III), once capped, would remain more strain-relaxed than QD's grown on an unstrained GaAs surface region. For a given composition and volume, this would imply a reduction of the band gap and a slight increase in the confinement energies. The QD's investigated here are relatively large and the reduction of the band gap (due to strain relaxation) will dominate over the confinement effect, and should result in a redshift of the PL emission. This is the opposite to what we observe and a strain-induced change in the band gap cannot explain the results observed here.

The most plausible explanation is a difference in the degree of intermixing during capping for these three types of QD's. Schmidt and Eberl¹⁰ reached the same conclusion for the Ge/Si QD system, where a detailed qualitative description of these mechanisms was presented. The same arguments apply to our bilayer InAs/GaAs QD structures. Following their model, we propose that QD's of types II and III are more strain relaxed than those of type I. When they are capped with GaAs, the strain gradient is much larger and this enhances the In/Ga intermixing as a way of releasing strain energy. As a consequence, the buried QD's are more intermixed and have a lower In composition after capping; hence the blueshift in the PL emission. This also provides an explanation for the differences observed between type-II and -III dots. In both cases, θ_{crit} is reduced compared to first-layer QD growth, suggesting that the strain fields from the underlying QD's extend through the spacer layer to create a

strain modulation on the surface. However, the surface morphology is very different with islands forming on mounds for the nonannealed case as opposed to a flat surface for the annealed spacer.^{18,25} The difference in surface morphology translates into a higher PL peak energy for the type-II dots. We believe this is again a result of enhanced intermixing during capping of the QD's when they are more strain-relaxed. Although the tensile strain is present in both cases, the presence of mounds probably enables the lattice constant to be even larger than on the flat (tensile strained) surface, resulting in type-II dots being more strain relaxed before capping than type-III dots, and therefore undergoing more intermixing during the capping stage. Future high-resolution TEM images of uncapped type-II and -III QD's should confirm this interpretation.

IV. CONCLUSIONS

We have presented a detailed study of the properties of bilayer InAs/GaAs QD's grown by molecular-beam epitaxy. STM measurements show that for a nonannealed GaAs spacer layer there is a reduction in the second-layer QD number density, which is accompanied by an increase in QD size. For a similar amount of InAs in the first and second layers (2.5 ML) the emission of the second-layer QD's is blueshifted, but by depositing more InAs in the second layer it is possible to obtain a single emission peak. The origin of the blueshift is attributed to an increased amount of intermixing in the capping process for the more strain-relaxed QD's. Annealing the spacer layer is demonstrated to be very important in order to obtain a similar number density in the two layers. The significant changes in the capping layer surface morphology and strain after annealing also result in a reduction of the intermixing during capping of the second-layer QD's compared to the nonannealed spacer. The observed blueshift is accordingly reduced. All these mechanisms should be taken into account when fabricating multilayer QD samples for device applications.

ACKNOWLEDGMENTS

This work was supported by the EPSRC, UK, who also provided studentships for P.B.J. and T.J.K. G.R.B. is grateful to the Ramsay Memorial Trust for the provision of a Research Fellowship, funded in part by VG Semicon Ltd. (UK).

*Email address: t.jones@ic.ac.uk FAX: +44-20-7594-5801.

¹Y. Arakawa and H. Sakaki, *Appl. Phys. Lett.* **40**, 939 (1982).

²M. O. Lipinski, H. Schuler, O. G. Schmidt, K. Eberl, and N. Y. Jin-Phillipp, *Appl. Phys. Lett.* **77**, 1789 (2000).

³G. S. Solomon, J. A. Trezza, A. F. Marshall, and J. S. Harris, Jr., *Phys. Rev. Lett.* **76**, 952 (1996).

⁴R. Heitz, A. Kalburge, Q. Xie, M. Grundmann, P. Chen, A. Hoffmann, A. Madhukar, and D. Bimberg, *Phys. Rev. B* **57**, 9050 (1998).

⁵I. Mukhametzhanov, R. Heitz, J. Zeng, P. Chen, and A. Madhukar, *Appl. Phys. Lett.* **73**, 1841 (1998).

⁶S. Fafard, M. Spanner, J. P. McCaffrey, and Z. R. Wasilewski,

Appl. Phys. Lett. **76**, 2268 (2000).

⁷J. Urayama, T. B. Norris, B. Kochman, J. Singh, and P. K. Bhat-tacharya, *Appl. Phys. Lett.* **76**, 2394 (2000).

⁸P. Frigeri, A. Bosacchi, S. Franchi, P. Allegri, and V. Avanzini, *J. Phys. Chem.* **201/202**, 1136 (1999).

⁹M. Colocci, A. Vinattieri, L. Lippi, F. Bogani, M. Rosa-Clot, S. Taddei, A. Bosacchi, S. Franchi, and P. Frigeri, *Appl. Phys. Lett.* **74**, 564 (1999).

¹⁰O. G. Schmidt and K. Eberl, *Phys. Rev. B* **61**, 13 721 (2000).

¹¹Q. Xie, A. Madhukar, P. Chen, and N. P. Kobayashi, *Phys. Rev. Lett.* **75**, 2542 (1995).

¹²Y. Nakata, Y. Suigiyama, T. Futatsugi, and N. Yokoyama, *J. Cryst.*

- Growth **175/176**, 713 (1997).
- ¹³W. Wu, J. R. Tucker, G. Solomon, and J. S. Harris, *Appl. Phys. Lett.* **71**, 1083 (1997).
- ¹⁴B. Legrand, J. P. Nys, B. Grandider, D. Stievenard, A. Lemaitre, J. M. Gerard, and V. Thierry-Mieg, *Appl. Phys. Lett.* **74**, 2608 (1999).
- ¹⁵B. Lita, R. S. Goldman, J. D. Philips, and P. K. Bhattacharya, *Appl. Phys. Lett.* **74**, 2824 (1999).
- ¹⁶J. Tersoff, C. Teichert, and M. G. Lagally, *Phys. Rev. Lett.* **76**, 1675 (1996).
- ¹⁷C. Priester, *Phys. Rev. B* **63**, 153303 (2001).
- ¹⁸P. B. Joyce, T. J. Krzyzewski, P. H. Steans, G. R. Bell, J. H. Neave, and T. S. Jones, *J. Cryst. Growth* (to be published).
- ¹⁹O. G. Schmidt, O. Kienzle, Y. Hao, K. Eberl, and F. Ernst, *Appl. Phys. Lett.* **74**, 1272 (1999).
- ²⁰E. C. Le Ru, A. J. Bennett, C. Roberts, and R. Murray, *J. Appl. Phys.* **91**, 1365 (2002).
- ²¹M. Itoh, G. R. Bell, A. R. Avery, T. S. Jones, B. A. Joyce, and D. D. Vvedensky, *Phys. Rev. Lett.* **81**, 633 (1998).
- ²²P. B. Joyce, T. J. Krzyzewski, G. R. Bell, T. S. Jones, E. C. Le Ru, and R. Murray, *Phys. Rev. B* **64**, 235317 (2001).
- ²³G. R. Bell, J. G. Belk, C. F. McConville, and T. S. Jones, *Phys. Rev. B* **59**, 2947 (1999).
- ²⁴J. G. Belk, C. F. McConville, J. Sudijono, T. S. Jones, and B. A. Joyce, *Surf. Sci.* **387**, 283 (1997).
- ²⁵P. B. Joyce, T. J. Krzyzewski, G. R. Bell, and T. S. Jones, *Appl. Phys. Lett.* **79**, 3615 (2001).
- ²⁶P. B. Joyce, T. J. Krzyzewski, P. H. Steans, G. R. Bell, J. H. Neave, and T. S. Jones, *Surf. Sci.* **492**, 345 (2001).
- ²⁷P. B. Joyce, T. J. Krzyzewski, G. R. Bell, T. S. Jones, S. Malik, D. Childs, and R. Murray, *Phys. Rev. B* **62**, 10 891 (2000).
- ²⁸P. D. Siverns, S. Malik, G. McPherson, D. Childs, C. Roberts, R. Murray, B. A. Joyce, and H. Davock, *Phys. Rev. B* **58**, R10 127 (1998).
- ²⁹I. Kegel, T. H. Metzger, A. Lorke, J. Peisl, J. Stangl, G. Bauer, J. M. Garcia, and P. M. Petroff, *Phys. Rev. Lett.* **85**, 1694 (2000).